

# Observation of the Ankle and Evidence for a High-Energy Break in the Cosmic Ray Spectrum

R.U. Abbasi<sup>a</sup> T. Abu-Zayyad<sup>a</sup> J.F. Amman<sup>b</sup> G. Archbold<sup>a</sup>  
R. Atkins<sup>a</sup> J.A. Bellido<sup>c</sup> K. Belov<sup>a</sup> J.W. Belz<sup>d</sup> S. Ben Zvi<sup>e</sup>  
D.R. Bergman<sup>f</sup> G.W. Burt<sup>a</sup> Z. Cao<sup>a</sup> R.W. Clay<sup>c</sup> C.B. Connolly<sup>e</sup>  
W. Deng<sup>a</sup> B.R. Dawson<sup>c</sup> Y. Fedorova<sup>a</sup> J Findlay<sup>a</sup> C.B. Finley<sup>e</sup>  
W.F. Hanlon<sup>a</sup> C.M. Hoffman<sup>b</sup> G.A. Hughes<sup>f</sup> M.H. Holzscheiter<sup>b</sup>  
P. Hütemeyer<sup>a</sup> C.C.H. Jui<sup>a</sup> K. Kim<sup>a</sup> M.A. Kirn<sup>d</sup> E.C. Loh<sup>a</sup>  
M.M. Maestas<sup>a</sup> N. Manago<sup>h</sup> L.J. Marek<sup>b</sup> K. Martens<sup>a</sup>  
J.A.J. Matthews<sup>g</sup> J.N. Matthews<sup>a</sup> A. O'Neill<sup>e</sup> C.A. Painter<sup>b</sup>  
L. Perera<sup>f</sup> K. Reil<sup>a</sup> R. Riehle<sup>a</sup> M. Roberts<sup>g</sup> M. Sasaki<sup>h</sup>  
S.R. Schnetzer<sup>f</sup> K.M. Simpson<sup>c</sup> G. Sinnis<sup>b</sup> J.D. Smith<sup>a</sup>  
R. Snow<sup>a</sup> P. Sokolsky<sup>a</sup> C. Song<sup>e</sup> R.W. Springer<sup>a</sup> B.T. Stokes<sup>a</sup>  
J.R. Thomas<sup>a</sup> S.B. Thomas<sup>a</sup> G.B. Thomson<sup>f</sup> D. Tupa<sup>b</sup>  
S. Westerhoff<sup>e</sup> L.R. Wiencke<sup>a</sup> A. Zech<sup>f</sup>

<sup>a</sup>*University of Utah, Department of Physics and High Energy Astrophysics  
Institute, Salt Lake City, Utah, USA*

<sup>b</sup>*Los Alamos National Laboratory, Los Alamos, NM, USA*

<sup>c</sup>*University of Adelaide, Department of Physics, Adelaide, South Australia, Australia*

<sup>d</sup>*University of Montana, Department of Physics and Astronomy, Missoula,  
Montana, USA*

<sup>e</sup>*Columbia University, Department of Physics and Nevis Laboratory, New York,  
New York, USA*

<sup>f</sup>*Rutgers - The State University of New Jersey, Department of Physics and  
Astronomy, Piscataway, New Jersey, USA*

<sup>g</sup>*University of New Mexico, Department of Physics and Astronomy, Albuquerque,  
New Mexico, USA*

<sup>h</sup>*University of Tokyo, Institute for Cosmic Ray Research, Kashiwa, Japan*

The High Resolution Fly's Eye Collaboration

---

**Abstract**

We have measured the cosmic ray spectrum at energies above  $10^{17}$  eV using the two air fluorescence detectors of the High Resolution Fly’s Eye experiment operating in monocular mode. We describe the detector, PMT and atmospheric calibrations, and the analysis techniques for the two detectors. We fit the spectrum to models describing galactic and extragalactic sources. Our measured spectrum gives an observation of a feature known as “the ankle” near  $3 \times 10^{18}$  eV, and strong evidence for a suppression near  $6 \times 10^{19}$  eV.

---

## 1 Introduction

The highest energy cosmic rays yet detected, of energies up to and above  $10^{20}$  eV, are interesting in that they shed light on two important questions: how are cosmic rays accelerated in astrophysical sources, and how do they propagate to us through the cosmic microwave background radiation (CMBR)? The acceleration of cosmic rays to ultra high energies is thought to occur in extensive regions of high magnetic fields, regions which are expanding at relativistic velocities[1]. Such regions are rare and are to be counted among the most violent and interesting objects in the universe.

Once accelerated, interactions between the ultra high energy cosmic rays (UHECR) and the CMBR cause the cosmic rays to lose energy. The strongest energy loss mechanism comes from the production of pions in these CMBR interactions at UHECR energies above about  $6 \times 10^{19}$  eV. This energy loss mechanism produces the Greisen-Zatsepin-K’uzmin (GZK) suppression[2,3]. In addition,  $e^+e^-$  production in these

same interactions provides a somewhat weaker energy loss mechanism above a threshold of about  $5 \times 10^{17}$  eV. A third important energy-loss mechanism at all energies comes from universal expansion.

In previous publications[4,5], we have reported on our measurements of the cosmic ray spectrum using data collected independently, in monocular mode, by the two detectors of the High Resolution Fly’s Eye experiment (HiRes). We here report on an updated measurement of the flux of UHECR, covering an energy range from  $2.5 \times 10^{17}$  eV to over  $10^{20}$  eV, using a significantly larger data set for the HiRes-II detector. With the improved statistical power available in this data, we study two features in this spectrum: a break in the spectral slope at  $3 \times 10^{18}$  eV, called the “ankle”[6–8], and a steepening of the spectrum near the threshold for pion production.

The HiRes experiment performs a calorimetric measurement of the energy of cosmic rays. UHECR produce extensive air showers (EAS) when they enter the atmosphere. The HiRes detector collects the fluorescence light emitted by EAS as they propagate through the atmosphere. Charged particles in the shower ex-

---

<sup>1</sup> To whom correspondence should be addressed. E-mail: bergman@physics.rutgers.edu

cite nitrogen molecules which fluoresce in the ultraviolet (300 to 400 nm). The fluorescence yield is about five photons per minimum ionizing particle per meter of path length[9]. As an EAS propagates through the atmosphere, the detector measures the number of photons seen as a function of time and angle. From this information, we reconstruct the geometry of the shower and the solid angle subtended by the detector from each point of the shower. From the number of photons collected, we reconstruct the number of charged particles in the shower as a function of the depth of the atmosphere traversed. We integrate the energy deposited in the atmosphere[10] to find the energy of the primary cosmic ray.

UHECRs are thought to be protons or heavier nuclei up to iron. While nucleus-nucleus collisions are complex, the general features of the interaction can be understood in terms of a simple superposition model. In this model each nucleon generates an independent EAS. The superposition of many, lower energy showers will result in an EAS with different statistical properties than an EAS produced by one high energy proton. This allows one to measure the composition of the primary cosmic rays on a statistical basis.

## 2 The HiRes Detectors

The HiRes detectors have been described extensively elsewhere[11,12]. In brief, they consist of spherical mirrors, of area  $5.1 \text{ m}^2$ , which collect

the fluorescence light and focus it onto a cluster of 256 photomultiplier tubes arranged in a  $16 \times 16$  array. Each tube in the cluster views about one square degree of the sky. Time and pulse height information are collected from each tube. The HiRes detectors trigger on and reconstruct showers that occur within a radius of about 35 km.

The HiRes-I detector is located atop Little Granite Mountain on the U.S. Army Dugway Proving Ground in west-central Utah. It consists of 22 mirrors, and their associated phototube arrays, arranged in one ring, observing from 3 degrees to 17 degrees in elevation and providing almost complete coverage in azimuthal angle. The detector uses a sample-and-hold readout system which integrates phototube pulses for  $5.6 \mu\text{s}$ . This is long enough to collect the signal from all cosmic ray showers of interest.

The HiRes-II detector is located on Camel's Back Ridge, also on Dugway Proving Ground, about 12.6 km SW of HiRes-I. It consists of 42 mirrors, arranged in two rings, covering from 3 to 31 degrees in elevation and almost the whole azimuthal angle range. This detector uses a flash ADC (FADC) readout system with a 100 ns sampling time.

In this article, we present data collected from June 1997 to February 2003 for HiRes-I, and from December 1999 through September 2001 for HiRes-II. For HiRes-II, this is about four times the data that was reported on previously. We collect

data on nights when the moon is down for three hours or more. In a typical year each detector collects up to about 1000 hours of data.

The weather is clear about 2/3 of the time at the HiRes sites. Since the presence of clouds reduces the experiment's aperture, we record the cloud coverage by operator observations, infrared cameras, and internal evidence within the data (a cosmic ray shower emerging from a cloud has a distinct signature, as does an upward going, artificial light source when it enters a cloud). Only data from nights with good weather are used in our spectrum measurements.

### 3 Calibration

The two most important calibrations we perform are of the photomultiplier tube (PMT) gains[13], and of the clarity of the atmosphere[14]. We use a stable xenon flash lamp, carried to each detector and used to illuminate the photomultiplier array, to find PMT gains. The xenon lamp produces a light intensity of about 10 photons per  $\text{mm}^2$  at the face of the PMTs; this intensity is traceable to NIST-calibrated photodiodes and is stable to about 2%, flash-to-flash. Separate calibrations of PMT gains using photoelectron statistics and using the absolute light intensity of the xenon flash lamp agree within uncertainties. Xenon flash lamp data are collected about once a month. A second calibration system, using a frequency-tripled YAG laser, is used to monitor phototube gains on

a night-to-night basis. We estimate that the relative calibration techniques are accurate to about 3% with an absolute calibration uncertainty of about  $\pm 10\%$ .

The atmosphere is our calorimeter, but it is also the medium through which fluorescence light propagates to the detectors. To calculate the number of fluorescence photons emitted by a cosmic ray shower, we must understand the way in which the atmosphere scatters this light between the EAS and the detector. The molecular component of the atmosphere is quite constant, with only small seasonal variations, and the Rayleigh scattering it produces is well understood. The aerosol content of the atmosphere can vary considerably over time, and with it, the amount of light scattered and its angular distribution.

To measure these quantities, we perform an atmospheric calibration using YAG lasers operating at wavelength  $\lambda = 355 \text{ nm}$ . At each of our two sites, we have a steerable beam laser which is fired in a pattern of shots that covers the detector's aperture, and which is repeated every hour. The scattered light from a laser at one site is collected by the detector at the other site. The amount of detected light is then analyzed to determine the scattering properties of the atmosphere. The properties that we measure are the vertical aerosol optical depth (VAOD), the horizontal aerosol extinction length, and the aerosol scattering phase function (the angular distribution of the differential scattering cross section).

Because about half of the data from HiRes-I were collected before the lasers were installed, we use average values of the measured parameters in this analysis: a horizontal aerosol extinction length of 25 km (the average horizontal molecular extinction length is 17 km), an average phase function, and a VAOD of 0.04. The atmosphere at our sites is quite clear: the average atmospheric correction to an event's energy is about 10% (see below for the effect on flux measurements). We are most sensitive to the value of VAOD. The RMS of the VAOD distribution is 0.02, and we use this RMS value as a conservative estimate of the systematic uncertainty in this parameter.

#### 4 HiRes-II Data Analysis

The analysis of the HiRes-II monocular data has been described previously[5]. The data presented here were collected during 540 hours of good weather running, and consists of 21 million triggers, mostly of random sky noise and events generated by atmospheric lasers and other man-made light sources. Events were selected that satisfied the following criteria:

- Angular speed  $\leq 11^\circ \mu s^{-1}$
- Selected tubes  $\geq 6$
- Photoelectrons/degree  $\geq 25$
- Track length  $\geq 7^\circ$ , or  $\geq 10^\circ$  for events extending above  $17^\circ$  elevation
- Zenith angle  $\leq 80^\circ$
- In-plane angle  $\leq 130^\circ$
- In-plane angle uncertainty  $\leq$

- $30^\circ$
- $150 \leq X_{max} \leq 1200 \text{ g/cm}^2$ , and is within  $50 \text{ g/cm}^2$  of begin visible in detector
- Average Čerenkov Correction  $\leq 70\%$
- Geometry fit  $\chi^2/\text{d.o.f.} \leq 10$
- Profile fit  $\chi^2/\text{d.o.f.} \leq 10$
- Minimal trigger from signal tubes required after March 2001

The final event sample consisted of 2685 events covering an energy range from  $10^{17.2} \text{ eV}$  to  $10^{20.0} \text{ eV}$ .

The geometry of each event is reconstructed using the time and angle information from the hit PMTs. First a pattern recognition step is performed to choose phototubes that lie on a line both in angle and in time. Next the plane that contains both the shower and the detector is determined from the azimuth and elevation of hit tubes; the angle of the shower in this plane is determined from a fit to phototube time and angle information. The resolution of shower-detector plane determination is about  $0.6^\circ$ , and the in-plane angle uncertainty is  $5^\circ$  on average.

With the geometry determined, the profile of the number of charged particles in the shower is calculated from the phototube pulse heights. Corrections are made for atmospheric scattering of the light, and for other effects such as mirror reflectivity, phototube quantum efficiency, etc. A correction is made for the Čerenkov light produced by charged particles in the shower. Both direct and scattered Čerenkov light contribu-

tions to the light seen by the PMTs are calculated and subtracted. The resulting shower development profile, expressed as a function of slant depth, is fit to the Gaisser-Hillas parameterization[15] (this has been seen to fit UHE cosmic ray showers quite well [10,16]). We integrate over the Gaisser-Hillas function and multiply by the average energy loss rate of  $2.19 \text{ MeV/g/cm}^2$  to calculate the energy of the primary cosmic ray. We then correct for unobserved energy (mostly neutrinos and muons which hit the ground).

## 5 Monte Carlo Simulation

To calculate the aperture as a function of cosmic ray energy, a very accurate Monte Carlo simulation of the experiment was performed[5]. Two libraries of cosmic ray showers, one for proton primaries and one for iron primaries, were generated using the Corsika[17] EAS simulation program and QGSJet[18] hadronic generator. Events from these libraries were placed by a detector simulation in the vicinity of the HiRes-II detector. This program also simulated the fluorescence and Čerenkov light generated by the showers, and calculated how much of this light would have been collected by the detectors. A complete simulation of the optical path, trigger, and readout electronics was performed. This simulation followed the experimental conditions that pertained over the data-collection period. The result was written out in the same format as the

data and analyzed by the same data analysis program described above. The stereoscopic energy spectrum of the Fly’s Eye experiment[6], and the composition measurements made by the HiRes/MIA hybrid experiment[19] and by HiRes in stereo[20] were used as inputs.

To convince ourselves that the Monte Carlo simulation was accurate, we compare many Monte Carlo distributions of geometrical and kinematic variables to the data. The agreement in these comparisons is excellent and indicates that we understand our detector. Figure 1 shows the brightness of showers: the number of photoelectrons per degree of track. The agreement between the data and Monte Carlo simulation indicates that the same amount of light is collected in the Monte Carlo as in the data. Figure 2 shows the  $\chi^2$  of a fit to the time vs. angle plot from which we determine shower geometry. The agreement here indicates that the resolution of the Monte Carlo is the same as that of the data. Figure 3 shows a histogram of the number of events vs the logarithm of their energy in EeV. The agreement here shows that, when we use previous measurements of the spectrum and composition in the Monte Carlo, and a complete simulation of the acceptance, we reproduce the experiment’s energy dependence.

## 6 HiRes-I Analysis

The analysis of the HiRes-I monocular data has also been described

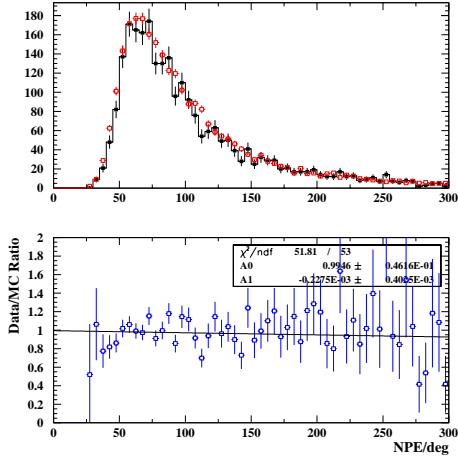


Fig. 1. Comparison of HiRes-II data and MC for the photoelectrons per degree of track. In the upper frame, the filled squares with the histogram are the data, the open squares are the MC. The lower frame shows the ratio of data to MC for each bin.

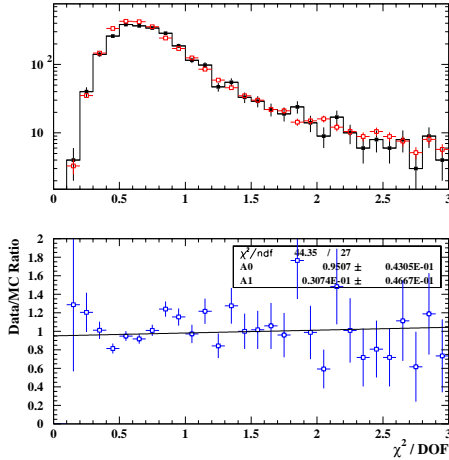


Fig. 2. Comparison of HiRes-II data and MC for the  $\chi^2$  of a fit to the time vs angle plot assuming a vertical shower. In the upper frame, the filled squares with the histogram are the data, the open squares are the MC. The lower frame shows the ratio of data to MC for each bin.

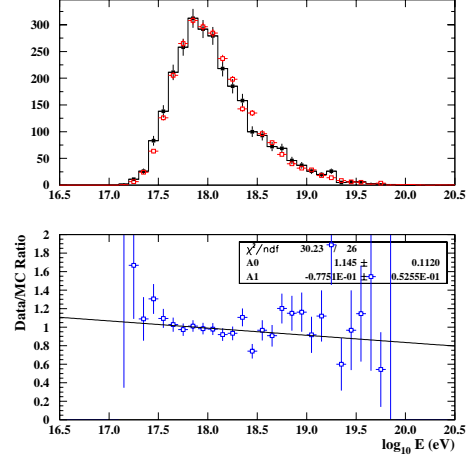


Fig. 3. Comparison of HiRes-II data and MC for the reconstructed energy. In the upper frame, the filled squares with the histogram are the data, the open squares are the MC. The lower frame shows the ratio of data to MC for each bin.

previously [4,5]. The main difference from the HiRes-II analysis is that, with only one ring of mirrors, most tracks are too short to reliably determine the geometry from timing alone. Although the determination of the shower-detector plane is still excellent, correlations between the fit distance to the shower and the fit in-plane angle become large for short tracks.

A reconstruction procedure using the pulse height information in addition to the tube angles and timing information has been developed: the profile constrained fit (PCF). The PCF uses the one-to-one correlation between in-plane angle and shower profile: the in-plane angle with the best fit shower profile is chosen as the in-plane angle of the shower. The Gaisser-Hillas function is used in this profile fit. The PCF works poorly for

events close to the detector (within about 5 km), and for lower energy events (below  $3 \times 10^{18}$  eV), where less of the shower profile is seen. These events are excluded from the HiRes-I monocular sample. The PCF also works poorly if too much Čerenkov light contaminates the fluorescence signal; these events are cut also. In reconstructing Monte Carlo events, it is found that, even with these cuts, the resolution is somewhat worse than for HiRes-II, and that there is an energy bias.

Since stereo events are seen in both detectors, they have excellent geometrical determination using the intersection of the two shower-detector planes. For these events, comparison of the PCF reconstruction to the stereo reconstruction shows the same energy resolution and bias as seen in the Monte Carlo sample. Having confidence that we understand the PCF, we correct for the bias. Figure 4 shows the energy resolution of the PCF reconstruction for Monte Carlo events and for stereo events after the correction. The agreement is excellent.

Figure 5 shows comparisons between the HiRes-I data and the Monte Carlo simulation for the distance to the shower core of showers in three energy bands. Again the agreement is excellent.

## 7 Systematic Uncertainties

The largest systematic uncertainties are the absolute calibration of the

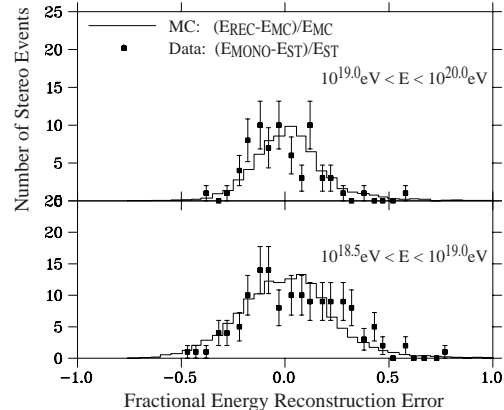


Fig. 4. Energy resolution using PCF, after bias correction. The histogram shows MC resolution, the data points show the data monocular resolution in stereo events.

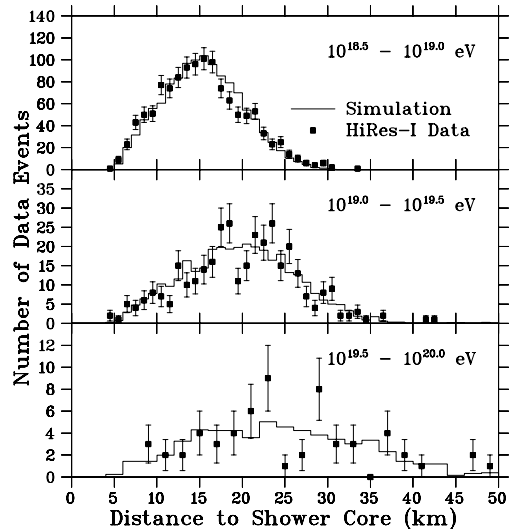


Fig. 5. Shower core distance distribution using PCF, in HiRes-I data and in MC. The squares with error bars are the data, the histogram is the MC.

phototubes ( $\pm 10\%$ ) [13], the fluorescence yield ( $\pm 10\%$ ) [9], the correction for unobserved energy in the shower ( $\pm 5\%$ ) [10], and the modeling of the atmosphere [14].

To test the sensitivity of the flux measurement to atmospheric uncertainties, we generated new Monte Carlo samples with VAOD values of

0.02 and 0.06, i.e., with the average plus and minus one RMS value, and analyzed them (and the data) using the same VAOD values. This provides a conservative estimate of the flux uncertainty since the systematic uncertainty in the average VAOD is less than the RMS. The result was a change in the flux of  $\pm 15\%$ . Adding this in quadrature with the other sources of systematic uncertainty results in a net uncertainty of  $\pm 31\%$ . This uncertainty is common to the flux measurements from HiRes-I and HiRes-II.

The limited elevation coverage of the HiRes-II detector makes the aperture calculation sensitive to the composition assumptions used in the Monte Carlo simulation. To estimate the uncertainty due to using the HiRes/MIA[19] and HiRes Stereo [20] composition measurements in our aperture calculation, we varied the overall proton fraction by  $\pm 5\%$ . This has a negligible effect on the aperture above an energy of  $10^{18}$  eV, and is of order the statistical error at  $3 \times 10^{17}$  eV[21].

## 8 Results

Figure 6 shows the aperture of the two HiRes detectors. At an energy of  $10^{20}$  eV the aperture is nearly 10,000  $\text{km}^2$  sr.

Figure 7 shows the measured spectrum of cosmic rays[22]. The spectrum has been multiplied by  $E^3$  for clarity. The closed squares (open circles) are the HiRes-I (HiRes-II) mea-

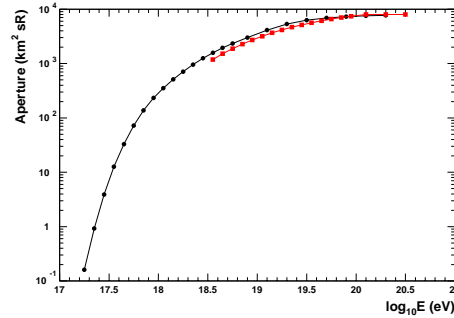


Fig. 6. The apertures of HiRes-I (red squares) and HiRes-II (black circles) as a function of energy.

surements. For comparison to previous experiments, the up-triangles are the stereo Fly’s Eye spectrum [6], and the down-triangles are the result of the Akeno Giant Air Shower Array (AGASA) [7]. The HiRes-I and HiRes-II monocular measurements agree with each other very well in the overlap region, and are also in good agreement with the Fly’s Eye stereo spectrum.

In this plot the ankle shows up clearly at  $10^{18.5}$  eV. The spectrum steepens again at  $10^{19.8}$  eV. The AGASA spectrum appears to continue unabated above this energy while the HiRes spectrum falls above this point.

We test whether our data are consistent with this interpretation of the AGASA spectrum by fitting our data to a broken power law. This fit is also shown on Figure 7. This fit had two floating break points separating three regions of constant spectral slope. The fitted break points are at  $\log_{10} E = 18.47 \pm 0.06$  eV and  $19.79 \pm 0.09$  eV. The fitted spectral slopes are  $\gamma = 3.32 \pm 0.04$ ,  $2.86 \pm 0.04$ , and  $5.2 \pm 1.3$ . If we extend the middle

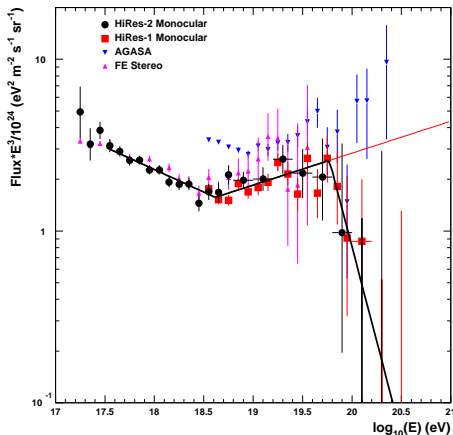


Fig. 7.  $E^3$  times the UHECR Flux. Results from the HiRes-I (red squares) and HiRes-II (black circles) detectors, the AGASA experiment (blue down-triangles) and the Fly’s Eye experiment (in stereo mode; magenta up-triangles) are shown. Also shown is a spectral law fit to the HiRes-I and HiRes-II spectra as described in the text. The  $1\sigma$  upper limits for two empty bins of each HiRes spectra are also shown.

section of the fit to higher energies our aperture predicts that we should have 28.0 events, where we really have 11. The Poisson probability for 11 or fewer events with a mean of 28 is  $2.4 \times 10^{-4}$ . We therefore conclude that our data is not consistent with a continuation of the spectrum unabated above the pion production threshold. It is worth emphasizing that we have considerable sensitivity to such a continuation, but the data do not support it.

A similar fit with only one break point has a worse  $\chi^2$  by 16. The fitted break point is at  $\log_{10} E = 18.45 \pm 0.03$  eV, and the fitted spectral slopes are  $\gamma = 3.32 \pm 0.03$  and

$2.85 \pm 0.05$ .

## 9 Fitting the Spectrum

The implications of our spectrum measurement can be explored using a toy model of UHECR. In this model, there are two types of sources, galactic and extragalactic. We choose the galactic sources to be consistent with the HiRes/MIA and HiRes stereo composition measurements[19,20]: we assign the iron component of the cosmic ray flux to be galactic[23]. This assignment is consistent with the expectation that the highest energy galactic cosmic rays should be those of the highest charge. The proton component we take to be extragalactic.

To describe the extragalactic cosmic rays, we assume that all sources have the same power law spectrum, and that cosmic rays lose energy in propagating to the earth by pion and  $e^+e^-$  production from the CMBR photons, and by the cosmological red shift[25]. Figure 8 shows our spectrum result with one fit superimposed on it. The fit includes the Hubble expansion, where source density follows changes in the volume of the universe. Here we multiply the density by  $(1+z)^m$ , where  $z$  is the redshift to the source and  $m = 3$ . The fitted value of  $-\gamma$ , the spectral slope of the spectrum at the source, is  $-\gamma = 2.32 \pm 0.01$ .

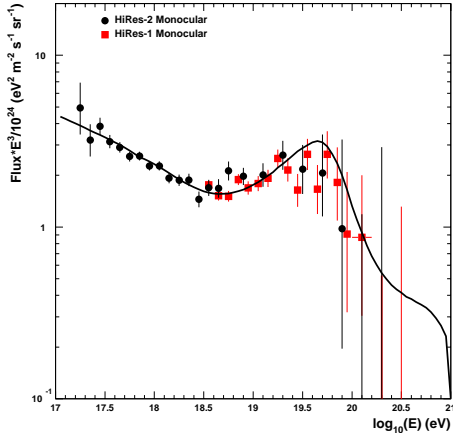


Fig. 8.  $E^3$  times the UHECR Flux. Results from the HiRes-I (red squares) and HiRes-II (black circles) detectors are shown. Also shown is a fit to a model described in the text. The  $1\sigma$  upper limits for two empty bins of each HiRes spectra are also shown.

## 10 Summary

We have measured the flux of ultra-high energy cosmic rays from  $10^{17.2}$  eV to over  $10^{20}$  eV. Our experiment detects atmospheric fluorescence light from cosmic ray showers and performs a calorimetric measurement of cosmic ray energies. We perform calibrations of our detector and measure the light-scattering properties of the atmosphere. The total systematic uncertainty in our spectrum measurement averages 31%.

In our energy range we observe two features in the UHECR spectrum visible through changes in the spectral power law. We observe the ankle at  $10^{18.6}$  eV. We also have evidence for a suppression at a higher energies, above  $10^{19.8}$  eV.

This work is supported by US NSF

grants PHY-9321949, PHY-9322298, PHY-0098826, PHY-0245428, PHY-0305516, PHY-0307098, by the DOE grant FG03-92ER40732, and by the Australian Research Council. We gratefully acknowledge the contributions from the technical staffs of our home institutions and the Utah Center for High Performance Computing. The cooperation of Colonels E. Fischer and G. Harter, the US Army, and the Dugway Proving Ground staff is greatly appreciated.

## References

- [1] R.J. Protheroe, Topics in Cosmic Ray Astrophysics (ed. M.A. DuVernois, Nova Science Publishing, NY, 1999) and astro-ph/9812055.
- [2] K. Greisen, Phys. Rev. Lett. **16**, 748, (1966).
- [3] G.T. Zatsepin and V.A. K'uzmin, Pis'ma Zh. Eksp. Teor. Fiz. **4**, 114 (166) [JETP Lett. **4**, 78 (1966)].
- [4] R. Abassi *et al.*, Phys. Rev. Lett. **92**, 151101, (2004).
- [5] R. Abassi *et al.*, to appear in Astropart. Phys., astro-ph/0208301.
- [6] D.J. Bird *et al.*, Phys. Rev. Lett. **71**, 3401, (1993).
- [7] M. Takeda *et al.*, Astropart. Phys. **19**, 447, (2003).
- [8] M. Ave *et al.*, Astropart. Phys. **19**, 47,
- [9] F. Kakimoto *et al.*, NIM A **372**, 527 (1996).

- [10] C. Song, Z. Cao *et al.*, *Astropart. Phys.* **14**, 7, (2000).
- [11] T. Abu-Zayyad *et al.*, *Proc. 26th Int. Cosmic Ray Conf. (Salt Lake City)*, **5**, 349, (1999).
- [12] J. Boyer, B. Knapp, E. Mannel, and M. Seman, to be published in NIM.
- [13] T. Abu-Zayyad *et al.*, to be submitted to NIM.
- [14] T. Abu-Zayyad *et al.*, in preparation.
- [15] T. Gaisser and A.M. Hillas, *Proc. 15th Int. Cosmic Ray Conf. (Plovdiv)*, **8**, 353, (1977).
- [16] T. Abu-Zayyad *et al.*, *Astropart. Phys.* **16**, 1, (2001).
- [17] D. Heck, J. Knapp, J.N. Capdevielle, G. Schatz and T. Thouw "CORSIKA : A Monte Carlo Code to Simulate Extensive Air Showers", Report FZKA 6019 (1998), Forschungszentrum Karlsruhe.
- [18] N.N. Kalmykov, S.S. Ostapchenko and A.I. Pavlov, *Nucl. Phys. B (Proc. Suppl.)* **52B**, 17, (1997).
- [19] T. Abu-Zayyad *et al.*, *Phys. Rev. Lett.* **84**, 4276, (2000).
- [20] R. Abbasi *et al.*, submitted to *Ap. J.*, astro-ph/0407622.
- [21] A. Zech, *Proc. of the Cosmic Ray Int. Sem. (CRIS'04)*, astro-ph/0409140.
- [22] The spectrum is available in tabular form at <http://www.cosmic-ray.org/ds123table.html>.
- [23] E. Waxman, *Astrophys. J. Lett.* **452**, L1, (1995); J.N. Bahcall and E. Waxman, *Phys. Lett.* **B556**, 1 (2003).
- [24] J. Linsley, *Proc. 18th Int. Cosmic Ray Conf. (Bangalore)*, **12**, 135, (1983).
- [25] V. Berezhinsky, A.Z. Gazizov, S.I. Grigorieva, hep-ph/0204357; S.T. Scully and F.W. Stecker, *Astropart. Phys.* **16**, 271, (2002); De Marco, Blasi, Olinto, *Astropart. Phys.* **20** (2003) 53.